

# ITINERANT FERROMAGNETISM AND SUPERCONDUCTIVITY

Naoum Karchev[\*]

November 20, 2018

Superconductivity has again become a challenge following the discovery of unconventional superconductivity. Resistance-free currents have been observed in heavy-fermion materials, organic conductors and copper oxides. The discovery of superconductivity in a single crystal of  $UGe_2$ ,  $ZrZn_2$  and  $URhGe$  revived the interest in the coexistence of superconductivity and ferromagnetism. The experiments indicate that: i) The superconductivity is confined to the ferromagnetic phase. ii) The ferromagnetic order is stable within the superconducting phase (neutron scattering experiments). iii) The specific heat anomaly associated with the superconductivity in these materials appears to be absent. The specific heat depends on the temperature linearly at low temperature.

I present a review of the recent experimental results and the basic theoretical ideas concerning ferromagnetic superconductivity (FM-superconductivity) induced by ferromagnetic spin fluctuations. A particular attention is paid to the magnon exchange mechanism of FM-superconductivity.

## 1 Introduction

The discovery of unconventional superconductivity caused an explosive growth of activities in various fields of condensed-matter research, stimulating not only studies of the basic mechanisms leading to this phenomenon, but also a widespread search for new technological applications. Resistance-free currents have been observed in heavy-fermion materials  $CeCu_2Si_2$ [1],  $UBe_{13}$ [2],  $UPt_3$ [3], and  $U_{1-x}Th_xBe_{13}$ [4], in organic conductors [5, 6, 7], copper oxides[8, 9] and layered ruthenate  $Sr_2RuO_4$ [10]. The great interest in the unconventional superconductivity is in particular due to their rather different normal- and superconducting-state properties. The mechanism of superconductivity and symmetry of the order parameter are the main puzzling of on-going research.

The Cooper pairing of conducting electrons is characterized by the gap function  $\Delta_{\sigma,\sigma'}(\mathbf{p})$ , which is a  $2 \times 2$  matrix-valued function of the wave vector  $\mathbf{p}$ . There is a symmetry relation which follows from the anti-commutation of spin  $\frac{1}{2}$  fermions

$$\Delta_{\sigma,\sigma'}(\mathbf{p}) = -\Delta_{\sigma',\sigma}(-\mathbf{p}), \quad (1)$$

The inversion symmetry is expressed by

$$P\Delta_{\sigma,\sigma'}(\mathbf{p}) = \Delta_{\sigma,\sigma'}(-\mathbf{p}), \quad (2)$$

and the time reversal symmetry by

$$\begin{aligned} T\Delta_{\sigma,\sigma}(\mathbf{p}) &= \Delta_{-\sigma,-\sigma}^*(-\mathbf{p}), \text{ where } (\sigma) = (\uparrow, \downarrow) \text{ and } (-\sigma) = (\downarrow, \uparrow) \\ T\Delta_{\sigma,\sigma'}(\mathbf{p}) &= -\Delta_{\sigma',\sigma}^*(-\mathbf{p}), \text{ when } \sigma \neq \sigma'. \end{aligned} \quad (3)$$

One can represent the gap matrix in the form

$$\Delta_{\sigma,\sigma'}(\mathbf{p}) = i\Delta(\mathbf{p})(\tau_2)_{\sigma,\sigma'} + id_{\mu}(\mathbf{p})(\tau_{\mu}\tau_2)_{\sigma,\sigma'}. \quad (4)$$

where  $\tau_1, \tau_2$  and  $\tau_3$  are the Pauli matrices,  $\Delta(\mathbf{p})$  is spin singlet function and  $d_{\mu}(\mathbf{p})$  is spin triplet one. The singlet part of the gap is a symmetric function  $\Delta(-\mathbf{p}) = \Delta(\mathbf{p})$ , while the triplet part is an antisymmetric one  $d_{\mu}(-\mathbf{p}) = -d_{\mu}(\mathbf{p})$ .

In conventional superconductors, the quasi-particles form Cooper pairs in a spin-singlet state  $\Delta(\mathbf{p}) \neq 0$ ,  $d_{\mu}(\mathbf{p}) = 0$ , which has zero total spin. The existence of the gap in the quasi-particle spectrum leads to unusual thermodynamic properties of the systems: i) The specific heat decreases exponentially as  $\exp(-\Delta(0)/k_B T)$  at low temperature, as opposed to the linear temperature dependence in the Fermi liquid theory[11]. ii) The same anomalous temperature dependence shows the paramagnetic susceptibility in s-type superconductors[12]. In the case of the singlet s-pairing, the nuclear spin-lattice relaxation rate  $1/T_1$  exhibits a peak just below the superconducting transition temperature[13]. Finally, the time-reversal and parity symmetries are not broken in conventional superconductors. All these properties are well understood on the basis of the Bardeen, Cooper, Schrieffer (BCS) theory of superconductivity[14]

Alternatively, the quasi-particles can form Cooper pairs in a spin-triplet state  $\Delta(\mathbf{p}) = 0$ ,  $d_{\mu}(\mathbf{p}) \neq 0$ , analogous to the "p-wave" state of paired neutral fermions in superfluid  $^3\text{He}$ [15]. At present, the heavy fermion compound  $UPt_3$  and layered ruthenate  $Sr_2RuO_4$  are the only known spin-triplet superconductors. The most direct way to identify the spin state of Cooper pairs is from measurements of their spin susceptibility, which can be determined by the Knight shift[16], and from measurements of nuclear spin-lattice relaxation rate  $1/T_1$ , probed by nuclear magnetic resonance and nuclear quadrupole resonance. No change in spin susceptibility was observed on passing through the superconducting transition in layered perovskite  $Sr_2RuO_4$ [16], and  $UPt_3$ [17, 18]. The relaxation rate  $1/T_1$  measured in  $Sr_2RuO_4$ [19] did not show coherence peak. Muon spin-relaxation measurements, for the same materials, reveal the spontaneous appearance of an internal magnetic field below the transition temperature. The appearance of such a field indicates that superconducting state is characterized by the breaking of time-reversal symmetry[20]. The unconventional nature of the superconductivity in  $UPt_3$  is confirmed by the observation of three superconducting phases denoted as A, B, and C in the  $H$ (magnetic field)- $T$ (temperature) phase diagram. Phases meet each other at a tetracritical point[21].

On theoretical ground, the unconventional superconductivity was described as a spin-triplet superconductivity: non-unitary spin-triplet superconductivity in  $UPt_3$ [22], and odd pairing state, which is two-dimensional analogue of the Balian-Werthamer state of  $^3He$ , in  $Sr_2RuO_4$ [23]. The non-unitary spin-triplet is defined by spin-1 complex vectorial function  $\mathbf{d}(\mathbf{p})$  which satisfy  $\mathbf{d}^*(\mathbf{p}) \times \mathbf{d}(\mathbf{p}) \neq 0$ . A test for odd-triplet pairing was proposed by T.M.Rice and M.Sigrist[23]. They consider a sandwich of thin film of  $Sr_2RuO_4$  between two singlet superconductors with higher transition temperature. Above  $T_{sc}$  of  $Sr_2RuO_4$  this system should behave like a standard SNS Josephson junction where the coupling is due to proximity-induced singlet pairs in  $Sr_2RuO_4$ . Below  $T_{sc}$ , however, the Josephson coupling should decrease because as triplet pairing appears in  $Sr_2RuO_4$  the proximity-induced singlet pairing will be suppressed. The anomalous temperature dependence of the Josephson effect would confirm the odd-parity symmetry of the order parameter in  $Sr_2RuO_4$ .

The discovery of superconductivity in a single crystal of  $UGe_2$ [24],  $ZrZn_2$ [25] and  $URhGe$ [26] revived the interest in the coexistence of superconductivity and ferromagnetism. The experiments indicate that: i)The superconductivity is confined to the ferromagnetic phase. ii)The ferromagnetic order is stable within the superconducting phase (neutron scattering experiments). iii)The specific heat anomaly associated with the superconductivity in these materials appears to be absent. The specific heat depends on the temperature linearly at low temperature.

The interplay of superconductivity and magnetism has a long history. The possible coexistence of superconductivity and ferromagnetism was considered as a theoretical possibility for weak itinerant ferromagnets many years ago[27]. In systems like  $ErRh_4B_4$ [28, 29] and  $HoMo_6S_8$ [30], it was observed that s-wave superconductivity gives way to ferromagnetism at intermediate temperatures. In all these compounds, superconductivity and magnetism originate from different part of the electron system. In contrast, in  $UGe_2$ ,  $ZrZn_2$ , and  $URhGe$  apparently the same band electrons are subject to the ferromagnetic and superconducting instability.

I present a review of the recent experimental results and the basic theoretical ideas concerning ferromagnetic superconductivity (FM-superconductivity) induced by ferromagnetic spin fluctuations. The review should be considered as a "progress report" in which I have attempted to focus on some basic aspects of this rapidly evolving field. Another goal of the review is to provide the reader with a simple overview of the experimental situation in ferromagnetic superconductors, summarizing the basic agreements and disagreements between theory and experiment. For additional literature the reader should consult other review articles[31].

The review is organized as follows. In the next section, a review of the experiments concerning  $UGe_2$ ,  $ZrZn_2$  and  $URhGe$  compounds is given. Theoretical models to describe superconductivity induced by spin fluctuations are presented in the third section. A particular attention is paid to the magnon exchange mechanism of FM-superconductivity.

## 2 Ferromagnetic superconductivity-experimental status

The coexistence of superconductivity and ferromagnetism has been studied for many years, but it has only recently been demonstrated to occur experimentally[24, 25, 26]. The most surprising fact is that the superconductivity occurs only in the ferromagnetic phase. The second surprise is that the specific heat anomaly associated with the superconductivity in these materials appears to be absent.

Recent experiments on single crystal[32] indicate that  $UGe_2$  has the base-centered orthorhombic crystal structure ( $Cmmm$ ) with zigzag chains of nearest-neighbor uranium ions. The structure is shown in Fig.1 taken from Ref.[33].

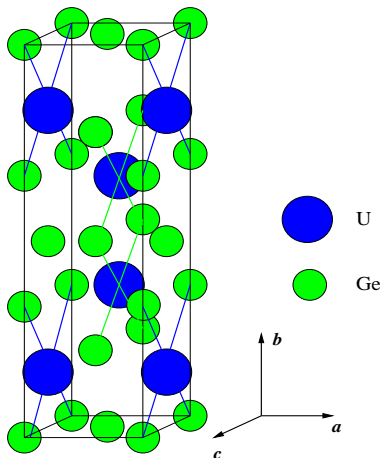


Figure 1: The base-centered orthorhombic  $Cmmm$  crystal structure of  $UGe_2$ .

In the uranium compounds known as "heavy-fermion systems" the  $5f$  electrons are highly localized and interact with fermions from more delocalized levels, giving rise to fermion excitations characterized by large effective masses. In  $UGe_2$ , however, the  $5f$  electrons are more itinerant than in many heavy-fermion systems. Specific heat measurements show that  $\gamma$  coefficient  $\gamma = C(T)/T$  is about 10 times smaller than in conventional heavy-fermion  $U$ -compounds ( $\gamma \approx 35 mJ/K^2$ [34]), which suggests that these electrons behave more like the  $3d$  electrons in the traditional itinerant ferromagnets such as  $Fe$ ,  $Co$  and  $Ni$ .  $UGe_2$  differs from the  $3d$  metals mainly in having a stronger spin orbit interaction that leads to an unusually large magnetocrystalline anisotropy with easy magnetization axis along  $\hat{a}$  (shortest crystallographic axis, Fig.1).

At ambient pressure  $UGe_2$  is an itinerant ferromagnet below the Curie temperature  $T_c = 52K$ , with low-temperature ordered moment of  $\mu_s = 1.4\mu_B/U$ . With increasing pressure the system passes through two successive quantum phase transition, from ferromagnetism to FM-superconductivity at  $P \sim 10$  kbar, and at higher pressure  $P_c \sim 16$  kbar to paramagnetism[24, 35]. The resulting

pressure  $p$  temperature  $T$  phase diagram for  $UGe_2$  is shown in Fig.2(a) taken from Ref.[35].

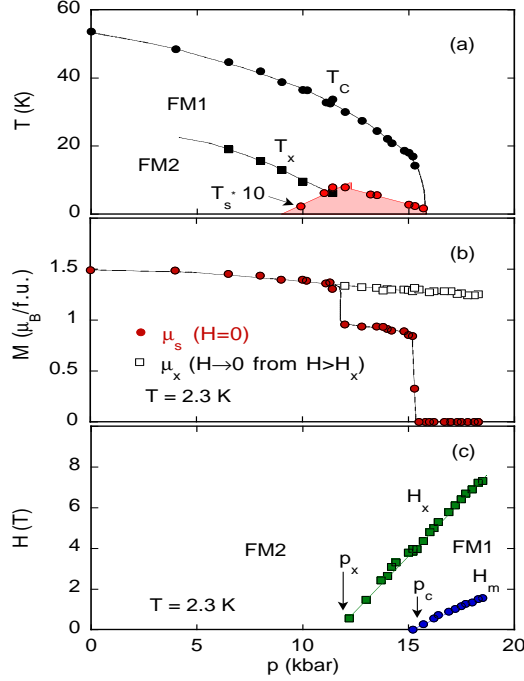


Figure 2: (a) The  $p$ – $T$  phase diagram of  $UGe_2$ .  $T_c$  is the Curie temperature  $T_s$  is the superconducting temperature. (b) Pressure dependence of  $\mu$  at  $T = 2.3$  K (full circles). The moment obtained by extrapolating the data from above  $H_x$  to zero (squares). (c) Pressure dependence of the fields  $H_x$  and  $H_m$  of metamagnetic transitions (at which  $dM/dH$  has a local maximum) at  $T = 2.3$  K

At the pressure where the superconducting transition temperature is a maximum  $T_{sc} = 0.8$  K, the ferromagnetic state is still stable with  $T_c = 32$  K, and the system undergoes a first order metamagnetic transition between two ferromagnetic phases  $FM2 \rightarrow FM1$  with different ordered moments [36]. The pressure dependence of the moment  $\mu$  at 2.3 K is shown in Fig.2(b) taken from Ref.[36]. (The symbol  $M$  is used for the magnetization in an external field).

The survival of bulk ferromagnetism below  $T_{sc}$  has been confirmed directly via elastic neutron scattering measurements[35]. The specific heat coefficient  $\gamma = C/T$  increases steeply near 11 kbar and retains a large and nearly constant value[37].

The resistivity measurements reveal[35] the presence of an additional phase line that lies entirely within the ferromagnetic phase. It is suggested by a strong anomaly seen in the resistivity. The characteristic temperature of this transition,  $T_x(p)$ , decreases with pressure and disappears at a pressure  $p_x$  close to the

pressure at which the superconductivity is strongest (Fig2(a)). The additional phase transition demonstrates itself and through the change in the  $T$  dependence of  $\mu(T)$ [36, 37]. In Fig.3, taken from[36], the temperature dependence of the ordered magnetic moment, is shown. A clear change in the  $T$  dependence of  $\mu(T)$  occurs at  $T_x$ .

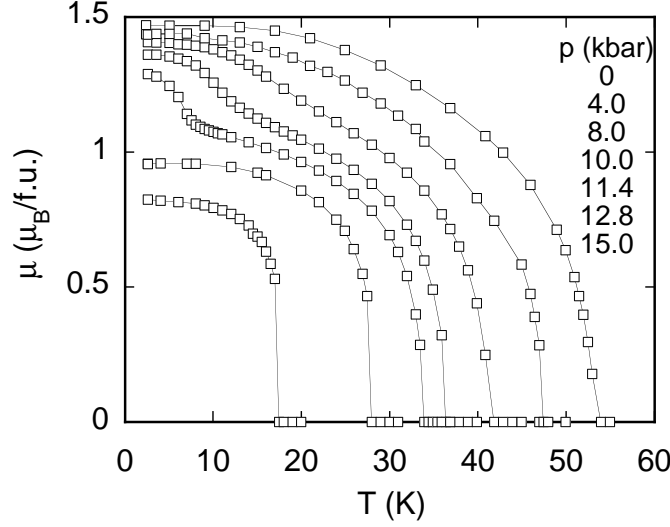


Figure 3: Temperature dependence of the ordered ferromagnetic moment. Curves correspond from top to bottom to the pressures indicated in the top right corner of the frame.

The field dependence of magnetization at  $2.3K$  for different  $p$  is shown in Fig.4, taken from[36]. For pressure  $p > p_x$  a large increase in the magnetization is observed at a field  $H_x$ . It is defined as the field at which  $dM/dH$  has a local maximum. It is plotted as a function of pressure in Fig.2(c). For  $p > p_c$  the magnetization undergoes a second increase at low field  $H_m$  corresponding to the paramagnetic  $\rightarrow$  ferromagnetic transition.

It is important to stress that the longitudinal uniform susceptibility, given by the slope  $dM/dH$  at  $H = 0$ , is small at a pressure  $p_x$  close to the pressure at which the superconductivity is strongest, and increases rapidly with increasing of  $p$ , while the superconducting transition temperature decreases. This experimental observation suggests that the longitudinal spin fluctuations suppress the formation of Cooper pairs.

The anomaly at  $T_x$  is quite similar to that observed in  $\alpha$  uranium. For  $\alpha$  uranium, there is direct evidence that the anomalies are due to the formation of charge density wave (CDW), resulting from nesting at the Fermi surface. Although band structure calculations[33, 38] indicate that a spin-majority Fermi surface sheet could become nested as a function of the magnetic polarization,

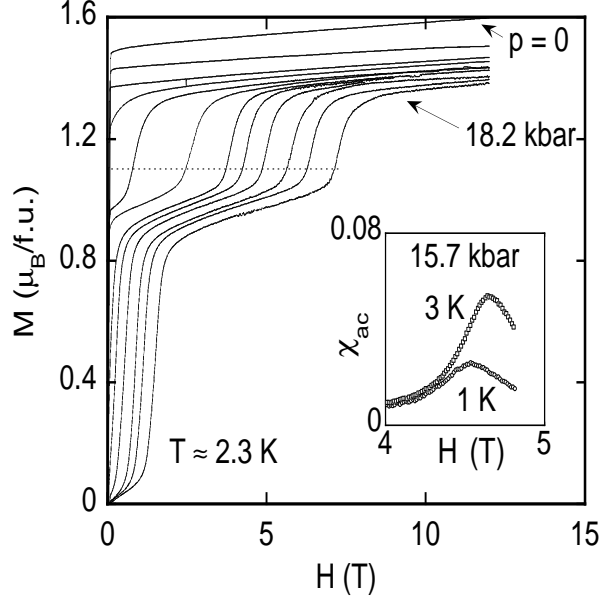


Figure 4: The field dependence of the easy-axis magnetization at 2.3K. Curves correspond from top to bottom to  $p=0, 6.5, 9.0, 11.1, 12.8, 15.3, 15.5, 16.0, 16.7, 17.3$ , and 18.2 kbar. The inset shows the ac susceptibility.

no direct evidence for a charge density or spin density wave has been found in neutron diffraction studies[39].

The studies of poly-crystalline samples of  $UGe_2$  show that T-P phase diagram is very similar to those of single-crystal specimens of  $UGe_2$ [40]. This result suggests that high-purity specimens with long mean free paths are not necessary, at least in the case of  $UGe_2$ , in order to observe superconductivity.

It is much less known about the  $ZrZn_2$  and  $URhGe$  compounds. The ferromagnets  $ZrZn_2$  and  $URhGe$  are superconducting at ambient pressure with superconducting critical temperatures  $T_{sc} = 0.29K$ [25] and  $T_{sc} = 0.25K$ [26] respectively.  $ZrZn_2$  is ferromagnetic below the Curie temperature  $T_c = 28.5K$  with low-temperature ordered moment of  $\mu_s = 0.17\mu_B$  per formula unit, while for  $URhGe$   $T_c = 9.5K$  and  $\mu_s = 0.42\mu_B$ . The quadratic low-temperature dependence of the squared magnetization is characteristic of simple itinerant ferromagnetism[41]. The low Curie temperatures and small ordered moments indicate that compounds are close to a ferromagnetic quantum critical point.

The physical properties of  $URhGe$  at zero pressure closely resemble those of  $UGe_2$  at the high pressures where superconductivity is found. Although the space groups and detailed structures of  $URhGe$  and  $UGe_2$  are different, both structures are orthorhombic and contain zigzag chains of nearest-neighbor uranium ions. Neutron scattering experiments reveal that the magnetization is almost entirely attributable to uranium 5f electrons.

The observation of a large jump in the specific heat, at the same temperature as the onset of superconductivity, demonstrates that the transition to superconductivity in *URhGe* is a bulk phase transition. It also shows that superconductivity involves the same itinerant electrons that are responsible for ferromagnetism. At low temperature the specific heat coefficient  $\gamma$  is twice as smaller as in the ferromagnetic phase.

The superconductivity in *ZrZn<sub>2</sub>* has a number of remarkable features. First, it only appears to occur in high-purity single-crystal sample. Second, there is no superconducting anomaly in the specific heat. It means that the superconducting state is strongly gapless with large portion of the Fermi surface, or even all of it, surviving in the superconducting state. Third, in contrast to *U*-based compounds, the bands at the Fermi energy in *ZrZn<sub>2</sub>* are predominantly *Zr4d*, and magnetism and superconductivity result from the same *4d* electrons.

The observation of superconductivity in *UGe<sub>2</sub>*, *URhGe* and *ZrZn<sub>2</sub>* suggests that superconductivity could occur more generally in ferromagnets. The coexistence of superconductivity and ferromagnetism may thus be more common and consequently more important than hitherto realized.

### 3 Theory of ferromagnetic superconductivity

#### 3.1 Lattice theory of strongly correlated systems

It is generally agreed that the origin of ferromagnetism lies in the Coulomb interaction between electrons. The Hamiltonian for electrons with spin  $\sigma$  interacting via Coulomb interaction  $V(\mathbf{r} - \mathbf{r}')$  in the presence of ionic potential  $V^{ion}(\mathbf{r})$  has the form[42]

$$\hat{H} = \hat{H}_0 + \hat{H}_{int} \quad (5)$$

where

$$\hat{H}_0 = \sum_{\sigma} \int d^3r \hat{\Psi}_{\sigma}^{\dagger}(\mathbf{r}) \left[ -\frac{\hbar^2}{2m} \Delta + V^{ion}(\mathbf{r}) \right] \hat{\Psi}_{\sigma}(\mathbf{r}) \quad (6)$$

$$\hat{H}_{int} = \frac{1}{2} \sum_{\sigma\sigma'} \int d^3r \int d^3r' V(\mathbf{r} - \mathbf{r}') \hat{n}_{\sigma}(\mathbf{r}) \hat{n}_{\sigma'}(\mathbf{r}'). \quad (7)$$

In equations (6) and (7)  $\hat{\Psi}_{\sigma}(\mathbf{r})$ ,  $\hat{\Psi}_{\sigma}^{\dagger}(\mathbf{r})$  are electron field operators and  $\hat{n}_{\sigma}(\mathbf{r}) = \hat{\Psi}_{\sigma}^{\dagger}(\mathbf{r})\hat{\Psi}_{\sigma}(\mathbf{r})$  is the local density operator. The lattice potential  $V^{ion}(\mathbf{r})$  leads to a splitting of the parabolic dispersion into bands. The non-interacted problem is then characterized by the Bloch wave functions  $\Phi_{\alpha,\mathbf{p}}(\mathbf{r})$  and the band energies  $\epsilon_{\alpha}(\mathbf{p})$ , where  $\alpha$  is the band's index. One may introduce Wannier functions localized at the atomic position  $\mathbf{R}_i$  by the relation

$$\chi_{\alpha,i} = \frac{1}{\sqrt{N}} \sum_{\mathbf{p}} e^{-i\mathbf{p}\cdot\mathbf{R}_i} \Phi_{\alpha,\mathbf{p}}(\mathbf{r}), \quad (8)$$

where  $N$  is the number of lattice sites, and to define the creation and annihilation operators  $\hat{c}_{\alpha,i\sigma}^{\dagger}$ ,  $\hat{c}_{\alpha,i\sigma}$  for electrons with spin  $\sigma$  in the band  $\alpha$  at site  $\mathbf{R}_i$  by the



equations

$$\hat{c}_{\alpha i \sigma} = \int d^3 r \chi_{\alpha, i}^*(\mathbf{r}) \hat{\Psi}_{\sigma}(\mathbf{r}) \longleftrightarrow \hat{\Psi}_{\sigma}(\mathbf{r}) = \sum_{i\alpha} \chi_{\alpha i}(\mathbf{r}) \hat{c}_{\alpha i \sigma}. \quad (9)$$

$$\hat{c}_{\alpha i \sigma}^+ = \int d^3 r \chi_{\alpha, i}(\mathbf{r}) \hat{\Psi}_{\sigma}^+(\mathbf{r}) \longleftrightarrow \hat{\Psi}_{\sigma}^+(\mathbf{r}) = \sum_{i\alpha} \chi_{\alpha i}^*(\mathbf{r}) \hat{c}_{\alpha i \sigma}^+. \quad (10)$$

After some algebra the Hamiltonian (5) may be rewritten in lattice representation, in terms of creation and annihilation operators

$$\hat{H} = \sum_{\alpha i j \sigma} t_{\alpha i j} \hat{c}_{\alpha i \sigma}^+ \hat{c}_{\alpha i \sigma} + \frac{1}{2} \sum_{\alpha \beta \gamma \delta} \sum_{i j m n} \sum_{\sigma \sigma'} V_{i j m n}^{\alpha \beta \gamma \delta} \hat{c}_{\alpha i \sigma}^+ \hat{c}_{\beta j \sigma'}^+ \hat{c}_{\delta n \sigma'} \hat{c}_{\gamma m \sigma}, \quad (11)$$

where the matrix elements are given by

$$t_{\alpha i j} = \int d^3 r \chi_{\alpha i}^*(\mathbf{r}) \left[ -\frac{\hbar^2}{2m} \Delta + V^{ion}(\mathbf{r}) \right] \chi_{\alpha j}(\mathbf{r}) \quad (12)$$

$$V_{i j m n}^{\alpha \beta \gamma \delta} = \int d^3 r \int d^3 r' \chi_{\alpha i}^*(\mathbf{r}) \chi_{\beta j}^*(\mathbf{r}') V(\mathbf{r} - \mathbf{r}') \chi_{\delta n}(\mathbf{r}') \chi_{\gamma m}(\mathbf{r}). \quad (13)$$

The Hamiltonian (11) is too general to be tractable. One may restrict the discussion to a single-band model ( $\alpha = \beta = \gamma = \delta = 1$ ). The advantage of the single-band model is its comparative mathematical simplicity. It is simple enough to handle in detail, but yet close enough to physical reality to supply with useful information, and the obtained effective model to be of general application. It is physically motivated to discuss this model if the Fermi surface lies within a single conduction band, and if this band is well separated from the other bands and the interaction is not too strong [42]. Accounting for the weak overlap between neighboring orbitals in tight-binding description one may restrict the sums over all sites of a lattice, to the sum over the nearest neighbors, denoted by  $\langle i, j \rangle$ . The remaining one-band, nearest-neighbor Hamiltonian has the form[42, 43, 44]

$$\begin{aligned} \hat{H} = & -t \sum_{\langle i, j \rangle \sigma} (\hat{c}_{i\sigma}^+ \hat{c}_{j\sigma} + h.c.) + U \sum_i \hat{n}_{i\uparrow} \hat{n}_{i\downarrow} + V \sum_{\langle i, j \rangle} \hat{n}_i \hat{n}_j \\ & - J \sum_{\langle i, j \rangle} \left( \hat{\mathbf{S}}_i \cdot \hat{\mathbf{S}}_j + \frac{1}{4} \hat{n}_i \hat{n}_j \right) \\ & + \sum_{\langle i, j \rangle} \left[ F \left( \hat{c}_{i\uparrow}^+ \hat{c}_{i\downarrow}^+ \hat{c}_{j\downarrow} \hat{c}_{j\uparrow} + h.c. \right) + X \sum_{\sigma} (\hat{c}_{i\sigma}^+ \hat{c}_{j\sigma} + h.c.) (\hat{n}_{i-\sigma} + \hat{n}_{j-\sigma}) \right]. \end{aligned} \quad (14)$$

where  $\hat{n}_i = \hat{n}_{i\uparrow} + \hat{n}_{i\downarrow}$  and  $S_i^{\mu} = 1/2 \sum_{\sigma \sigma'} \hat{c}_{i\sigma}^{\dagger} \tau_{\sigma \sigma'}^{\mu} \hat{c}_{i\sigma'}$ . The local(Hubbard) term describes the Coulomb repulsion ( $U > 0$ ), the J-term corresponds to the direct Heisenberg exchange which is generically ferromagnetic ( $J > 0$ ) in nature, the V-term describes the density-density interaction, the X-term is a density dependent hopping and, finally, the F-term describes the hopping of local pairs

consisting of an up and down electron. Coulomb repulsion  $U$  is the largest energy scale in the problem. In a final step one may neglect the nearest-neighbor interactions to obtain the simplest model of strongly correlated electrons, the Hubbard model[42].

### 3.2 Magnon-paramagnon effective theory

Theories of weak ferromagnetic metals have been developed by several theorists [45, 46, 47, 48, 49, 41, 50, 51]. The spectrum of the spin excitations has been found. It consists of spin fluctuations of paramagnon type and a transverse spin-wave branch. The present subsection is devoted to the derivation of an effective magnon-paramagnon theory starting from a microscopic single-band lattice model of ferromagnetic metals with Hamiltonian

$$\hat{H} = -t \sum_{\langle i,j \rangle, \sigma} (\hat{c}_{i\sigma}^\dagger \hat{c}_{j\sigma} + \text{h.c.}) - J \sum_{\langle i,j \rangle} \hat{\mathbf{S}}_i \cdot \hat{\mathbf{S}}_j + U \sum_i \hat{n}_{i\uparrow} \hat{n}_{i\downarrow} - \mu \sum_i \hat{n}_i, \quad (15)$$

where  $\mu$  is the chemical potential.

Given that the Hubbard coupling  $U$  is the largest energy scale in the theory it is desirable to diagonalize the Hubbard term. We should also define spin-wave excitations such that they are the true Goldstone modes. To accomplish both of these goals one introduces Schwinger-bosons  $(\hat{\varphi}_{i,\sigma}, \hat{\varphi}_{i,\sigma}^\dagger)$  and slave-fermions  $(\hat{h}_i, \hat{h}_i^\dagger, \hat{d}_i, \hat{d}_i^\dagger)$  representation for the operators

$$\begin{aligned} \hat{c}_{i\uparrow} &= \hat{h}_i^\dagger \hat{\varphi}_{i1} + \hat{\varphi}_{i2}^\dagger \hat{d}_i, & \hat{c}_{i\downarrow} &= \hat{h}_i^\dagger \hat{\varphi}_{i2} - \hat{\varphi}_{i1}^\dagger \hat{d}_i, \\ \hat{c}_{i\uparrow}^\dagger \hat{c}_{i\uparrow} \hat{c}_{i\downarrow}^\dagger \hat{c}_{i\downarrow} &= \hat{d}_i^\dagger \hat{d}_i, & \hat{\vec{S}}_i &= \frac{1}{2} \sum_{\sigma\sigma'} \hat{\varphi}_{i\sigma}^\dagger \vec{\tau}_{\sigma\sigma'} \hat{\varphi}_{i\sigma'}, \\ \hat{n}_i &= 1 - \hat{h}_i^\dagger \hat{h}_i + \hat{d}_i^\dagger \hat{d}_i, & \hat{\varphi}_{i\sigma}^\dagger \hat{\varphi}_{i\sigma} + \hat{d}_i^\dagger \hat{d}_i + \hat{h}_i^\dagger \hat{h}_i &= 1 \end{aligned} \quad (16)$$

The partition function can be written as a path integral over the complex functions of the Matsubara time  $\tau$   $\varphi_{i\sigma}(\tau)$  ( $\bar{\varphi}_{i\sigma}(\tau)$ ) and Grassmann functions  $h_i(\tau)$  ( $\bar{h}_i(\tau)$ ) and  $d_i(\tau)$  ( $\bar{d}_i(\tau)$ ).

$$\mathcal{Z}(\beta) = \int D\mu (\bar{\varphi}, \varphi, \bar{h}, h, \bar{d}, d) e^{-S}. \quad (17)$$

The action is given by the expression

$$S = \int_0^\beta d\tau \left[ \sum_i \left( \bar{\varphi}_{i\sigma}(\tau) \dot{\varphi}_{i\sigma}(\tau) + \bar{h}_i(\tau) \dot{h}_i(\tau) + \bar{d}_i(\tau) \dot{d}_i(\tau) \right) + H(\bar{\varphi}, \varphi, \bar{h}, h, \bar{d}, d) \right], \quad (18)$$

where  $\beta$  is the inverse temperature and the Hamiltonian is obtained from Eqs.(15) and (16) replacing the operators with the functions. In terms of the Schwinger bosons and slave-fermions the theory is  $U(1)$  gauge invariant, and the measure includes  $\delta$  functions that enforce the constraint and the gauge-fixing condition

$$D\mu(\bar{\varphi}, \varphi, \bar{h}, h, \bar{d}, d) = \prod_{i, \tau, \sigma} \frac{D\bar{\varphi}_{i\sigma}(\tau) D\varphi_{i\sigma}(\tau)}{2\pi i} \prod_{i\tau} D\bar{h}_i(\tau) Dh_i(\tau) D\bar{d}_i(\tau) Dd_i(\tau) \prod_{i\tau} \delta(\bar{\varphi}_{i\sigma}(\tau)\varphi_{i\sigma}(\tau) + \bar{h}_i(\tau)h_i(\tau) + \bar{d}_i(\tau)d_i(\tau) - 1) \prod_{i\tau} \delta(g.f). \quad (19)$$

The ferromagnetic order parameter is a vector field  $\mathbf{M}$ . The transverse spin fluctuations (magnons) are described by  $(M_1 + iM_2)$  and  $(M_1 - iM_2)$  fields, and the longitudinal fluctuations (paramagnons) by  $M_3$ . Alternatively the vector field can be written as a product of its amplitude  $\rho = \sqrt{M_1^2 + M_2^2 + M_3^2}$  and an unit vector  $\mathbf{n}$ ,  $\mathbf{M} = \rho\mathbf{n}$ . In the ferromagnetic phase one sets  $M_3 = \langle M_3 \rangle + \varphi$  and in linear (spin-wave) approximation obtains  $\rho = \langle M_3 \rangle + \varphi$ . It is evident now, that the fluctuations of the  $\rho$  field,  $\rho - \langle M_3 \rangle$  are exactly the paramagnon excitations in a formalism which keeps  $O(3)$  symmetry manifest. One can write the effective theory in terms of  $\mathbf{M}$ -vector components, or, equivalently, in terms of  $\rho$  and an unit vector  $\mathbf{n}$ . I use the parametrization in terms of unit vector and spin singlet amplitude because the unit vector  $\mathbf{n}$  describes the true Goldstone modes of the order parameter. With that end in view I make a change of variables, introducing new Bose fields  $f_{i\sigma}(\tau)$  ( $\bar{f}_{i\sigma}(\tau)$ ) Ref.[52]

$$\begin{aligned} f_{i\sigma}(\tau) &= \varphi_{i\sigma}(\tau) [1 - \bar{h}_i(\tau)h_i(\tau) - \bar{d}_i(\tau)d_i(\tau)]^{-\frac{1}{2}}, \\ \bar{f}_{i\sigma}(\tau) &= \bar{\varphi}_{i\sigma}(\tau) [1 - \bar{h}_i(\tau)h_i(\tau) - \bar{d}_i(\tau)d_i(\tau)]^{-\frac{1}{2}}, \end{aligned} \quad (20)$$

where the new fields satisfy the constraint

$$\bar{f}_{i\sigma}(\tau)f_{i\sigma}(\tau) = 1. \quad (21)$$

In terms of the new fields the spin vector has the form

$$S_i^\mu(\tau) = \frac{1}{2} \sum_{\sigma\sigma'} \bar{f}_{i\sigma}(\tau) \tau_{\sigma\sigma'}^\mu f_{i\sigma'}(\tau) [1 - \bar{h}_i(\tau)h_i(\tau) - \bar{d}_i(\tau)d_i(\tau)] \quad (22)$$

where  $n_i^\mu = \sum_{\sigma\sigma'} \bar{f}_{i\sigma} \tau_{\sigma\sigma'}^\mu f_{i\sigma'}$  is a unit vector and  $[1 - \bar{h}_i(\tau)h_i(\tau) - \bar{d}_i(\tau)d_i(\tau)]$  is the spin-vector's amplitude. When the lattice site is empty or doubly occupied the spin vector is zero. When the lattice site is occupied by one electron the unit vector  $\mathbf{n}_i$  identifies the local orientation. One can consider the first two components  $n_{i1}$  and  $n_{i2}$  as independent, and then  $n_{i3} = \sqrt{1 - n_{i1}^2 - n_{i2}^2}$ . In the leading order of the fields, the spin vector has the form

$$S_{i1} \simeq \frac{1}{2}n_{i1}, \quad S_{i2} \simeq \frac{1}{2}n_{i2}, \quad S_{i3} - \frac{1}{2} \simeq -\frac{1}{2}(\bar{h}_i h_i + \bar{d}_i d_i). \quad (23)$$

The last equation shows that the longitudinal spin fluctuations are associated with the collective fields  $(\bar{h}_i h_i + \bar{d}_i d_i)$ . To avoid misunderstandings, it is important to point out that the charge-waves are associated with the collective field  $(\bar{d}_i d_i - \bar{h}_i h_i)$  (see the representation of the electron number operator (16)).

In terms of the new fields the action has the form

$$S = \int_0^\beta d\tau \left\{ \sum_i \left[ \bar{f}_{i\sigma}(\tau) \dot{f}_{i\sigma}(\tau) + \bar{h}_i(\tau) \left( \frac{\partial}{\partial \tau} - \bar{f}_{i\sigma}(\tau) \dot{f}_{i\sigma}(\tau) \right) h_i(\tau) + \bar{d}_i(\tau) \left( \frac{\partial}{\partial \tau} - \bar{f}_{i\sigma}(\tau) \dot{f}_{i\sigma}(\tau) \right) d_i(\tau) \right] + H(\bar{f}, f, \bar{h}, h, \bar{d}, d) \right\}, \quad (24)$$

where  $H(\bar{f}, f, \bar{h}, h, \bar{d}, d)$  is the Hamiltonian

To formulate a mean-field theory I drop the terms of order equal or higher than six in the Hamiltonian and decouple the four-fermion term, by means of the Hubbard-Stratanovich transformation, introducing a real, spin-singlet  $S_i(\tau)$  field, corresponding to the collective field  $(\bar{h}_i h_i + \bar{d}_i d_i)$ . Now, the action is quadratic with respect to the fermions and one can integrate them out. The resulting action depends on the spinons  $\bar{f}_{i\sigma}, f_{i\sigma}$  and the real field  $S_i$ . It has a minimum at the point  $S_i = s_0, f_{i\sigma} = f_\sigma$ , and the stationary condition is

$$s_0 = \langle \bar{h}_i h_i + \bar{d}_i d_i \rangle \quad (25)$$

Expanding the effective action around the mean field point one obtains the effective model in terms of the spinons  $\bar{f}_\sigma(\tau, \mathbf{r}), f_\sigma(\tau, \mathbf{r})$  and paramagnons  $\varphi_i(\tau)$  ( $2\varphi_i(\tau) = s_0 - S_i(\tau)$ )[53]. The first three terms in the expansion have the form

$$S_{eff} = S_H + S_p + S_{int}, \quad (26)$$

$S_H$  is the action of the Heisenberg theory of localized spins. In the continuum limit it has the form

$$S_H = \int_0^\beta d\tau \int d^3r \left[ 2M \bar{f}_\sigma(\tau, \mathbf{r}) \dot{f}_\sigma(\tau, \mathbf{r}) + \frac{M^2 J_r}{2} \sum_{\nu=1}^3 \partial_\nu \mathbf{n}(\tau, \mathbf{r}) \cdot \partial_\nu \mathbf{n}(\tau, \mathbf{r}) \right]. \quad (27)$$

In Eq.(27),  $M = \frac{1}{2}(1 - s_0)$ , and  $s_0$  comes from "tadpoles" diagrams with one  $h$  or  $d$  line, and the renormalized exchange coupling constant  $J_r$  is calculated in [53].

$S_p$  is the contribution to the effective action of the paramagnon excitations

$$S_p = \frac{1}{2} \int \frac{d\omega}{2\pi} \frac{d^3p}{(2\pi)^3} \varphi(\omega, \mathbf{p}) \left( r + a \frac{|\omega|}{p} + bp^2 \right) \varphi(-\omega, -\mathbf{p}) \quad (28)$$

where the constants are obtained from the Lindhard functions for  $h$  and  $d$  fermions in the limit when  $p$  and  $\frac{\omega}{p}$  are small.

Finally, the spinon-paramagnon interaction has the form

$$S_{int} = M^2 \lambda \int_0^\beta d\tau \int d^3r \varphi(\tau, \mathbf{r}) \left[ \sum_{\nu=1}^3 \partial_\nu \mathbf{n}(\tau, \mathbf{r}) \cdot \partial_\nu \mathbf{n}(\tau, \mathbf{r}) \right] \quad (29)$$

where the effective magnon-paramagnon coupling is obtained from triangular diagrams with two  $h$  and one  $d$  lines or with two  $d$  and one  $h$  lines.

To analyze the effective model, it is more convenient to rewrite it in terms of rescaled spinon fields

$$\bar{\zeta}_\sigma = \sqrt{2M}\bar{f}_\sigma, \quad \zeta_\sigma = \sqrt{2M}f_\sigma. \quad (30)$$

The new fields satisfy the constraint

$$\bar{\zeta}_\sigma \zeta_\sigma = 2M, \quad (31)$$

and the action of the effective theory has the form

$$\begin{aligned} S_{eff} = & \int_0^\beta d\tau \int d^3r \left[ \bar{\zeta}_\sigma(\tau, \mathbf{r}) \dot{\zeta}_\sigma(\tau, \mathbf{r}) + \frac{J_r}{2} \sum_{\nu=1}^3 \partial_\nu \mathbf{M}(\tau, \mathbf{r}) \cdot \partial_\nu \mathbf{M}(\tau, \mathbf{r}) \right. \\ & \left. + \frac{\lambda}{4} \varphi(\tau, \mathbf{r}) \left[ \sum_{\nu=1}^3 \partial_\nu \mathbf{M}(\tau, \mathbf{r}) \cdot \partial_\nu \mathbf{M}(\tau, \mathbf{r}) \right] \right] + S_p, \end{aligned} \quad (32)$$

where  $\mathbf{M}$  is the spin vector

$$M^\mu = \frac{1}{2} \bar{\zeta}_\sigma \tau_{\sigma, \sigma'}^\mu \zeta_{\sigma'}, \quad \mathbf{M}^2 = M^2 \quad (33)$$

and  $S_p$  is given by Eq.(28).

It follows from Eq.(22) that the dimensionless magnetization of the system, per lattice site is defined by the equation,

$$\langle S_i^3 \rangle = \frac{1}{2} \langle n_i^3 \rangle (1 - \langle \bar{h}_i h_i + \bar{d}_i d_i \rangle). \quad (34)$$

At zero temperature  $\langle n_i^3 \rangle = 1$  and using the Eq.(25) one obtains that  $M$  is zero temperature dimensionless magnetization of the system per lattice site,  $M = \langle S_i^3 \rangle$ . The parameter  $M$  depends on the microscopic parameters of the theory and characterizes the vacuum. If, in the vacuum state, every lattice site is occupied by one electron with spin up, then  $M = \frac{1}{2}$  ( $s_0 = 0$ ), the parameters  $a$  and  $b$  are equal to zero and  $r = \frac{3J}{2}$ . In this case one can integrate over the paramagnons and the resulting theory is the spin  $\frac{1}{2}$  Heisenberg theory of the localized spins. When, in the vacuum state, some of the sites are doubly occupied ( $\langle \bar{d}_i d_i \rangle \neq 0$ ) or empty ( $\langle \bar{h}_i h_i \rangle \neq 0$ ), then  $M < \frac{1}{2}$ , the relevant excitations are the spinon and paramagnon excitations and the effective theory is a "spin  $M$ " Heisenberg theory coupled to paramagnon fluctuations defined by Eqs.(31,32,33). The system approaches the quantum critical point when  $M \rightarrow 0$  ( $s_0 \rightarrow 1$ ), and  $r(M)$  approaches zero when  $M \rightarrow 0$ . Hence, the parameter  $r$  measures the distance from the quantum critical point. In quantum paramagnetic phase ( $M = 0$ ), the spinon excitations disappear from the spin spectrum (see Eqs.(31,33)) and one obtains Hertz's effective model[50]. (One

can add a four-paramagnon term, calculating one-loop diagrams with four  $h$  or  $d$  fermion lines, but I have dropped it motivated by the Hertz's result.)

In thermal paramagnetic phase (above Curie temperature) the spectrum consists of spin singlet fluctuations of paramagnon type and spin- $\frac{1}{2}$  spinon fluctuations. Well above the critical temperature the spinon has a large gap, and the physics of ferromagnetic metals is dominated by the paramagnon fluctuations. But just above  $T_c$  the spinon's gap approaches zero [54], and the contribution of the spin- $\frac{1}{2}$  fluctuations is essential.

Below the Curie temperature it is convenient to introduce explicitly the magnon excitations  $a(\tau, \mathbf{r})$ ,  $\bar{a}(\tau, \mathbf{r})$ . To this end, I consider the  $U(1)$  gauge invariant theory (32) and impose the gauge-fixing condition in the form  $\arg \zeta_1 = 0$ . Then the constraint (31) can be solved by means of the complex field  $a = \zeta_2$  and  $\zeta_1 = \sqrt{2M - \bar{a}a}$ . For the components of the spin vector  $M^+ = M_1 + iM_2$ ,  $M^- = M_1 - iM_2$ , and  $M_3$  one obtains the Holstein-Primakoff representation:

$$\begin{aligned} M^+ &= \sqrt{2M - \bar{a}a} a, \quad M^- = \bar{a} \sqrt{2M - \bar{a}a}, \\ M^3 &= M - \bar{a}a \end{aligned} \quad (35)$$

The kinetic term in the action and the measure are the same as the kinetic term and the measure in the theory of a Bose field. The only difference is that the complex fields are subject to the condition  $\bar{a}a \leq 1$ .

In the spin-wave theory one approximates  $\sqrt{2M - \bar{a}a}$  and integrates over the whole complex plane. Then, the model is simplified and the effective action can be written in terms of magnon  $\bar{a}$ ,  $a$  and paramagnon  $\varphi$  fields

$$\begin{aligned} S_{eff} &= \int \frac{d\omega}{2\pi} \frac{d^3p}{(2\pi)^3} [\bar{a}(\omega, \mathbf{p}) (i\omega + \rho p^2) a(\omega, \mathbf{p}) \\ &+ \frac{1}{2} \varphi(\omega, \mathbf{p}) \left( r + a \frac{|\omega|}{p} + bp^2 \right) \varphi(-\omega, -\mathbf{p})] \\ &+ \frac{m\lambda}{2} \int \prod_{l=1}^2 \frac{d\omega_l}{2\pi} \frac{d^3p_l}{(2\pi)^3} (\mathbf{p}_1 \cdot \mathbf{p}_2) \bar{a}(\omega_1, \mathbf{p}_1) a(\omega_2, \mathbf{p}_2) \varphi(\omega_1 - \omega_2, \mathbf{p}_1 - \mathbf{p}_2) \end{aligned} \quad (36)$$

where

$$\rho = M J_r \quad (37)$$

is the spin stiffness constant.

In the spin-wave approximation the transverse components of the spin fields are proportional to the magnon fields

$$S^+(\tau, \mathbf{r}) = \sqrt{2M} a(\tau, \mathbf{r}), \quad S^-(\tau, \mathbf{r}) = \sqrt{2M} \bar{a}(\tau, \mathbf{r}) \quad (38)$$

and the field  $\varphi(\tau, \mathbf{r})$  is exactly the paramagnon (longitudinal spin fluctuation)

$$S^3(\tau, \mathbf{r}) - \langle S^3 \rangle = \varphi(\tau, \mathbf{r}). \quad (39)$$

Hence, in Gaussian approximation, spin-spin correlation functions have the form

$$D^{tr}(\omega, \vec{p}) = \frac{2M}{i\omega + \rho p^2}, \quad D^{long}(\omega, \vec{p}) = \frac{1}{r + a \frac{|\omega|}{p} + bp^2}, \quad (40)$$

where the longitudinal magnetic susceptibility is

$$\chi = D^{long}(0, 0) = \frac{1}{r} \quad (41)$$

### 3.3 Spin-induced four-fermion interaction

The next step is to consider model which describes fermions interacting with their own collective spin fluctuations. The action of the effective spin-fermion theory has the form

$$\begin{aligned} S_{s-f} = & \int_0^\beta d\tau \int d^3r \left[ c_\sigma^+(\tau, \mathbf{r}) \left( -\frac{1}{2m} \Delta - \mu \right) c_\sigma(\tau, \mathbf{r}) \right. \\ & \left. + \frac{J}{2} c_\sigma^+(\tau, \mathbf{r}) \tau_{\sigma\sigma'}^\mu c_{\sigma'}(\tau, \mathbf{r}) S^\mu(\tau, \mathbf{r}) \right] + S_{eff}, \end{aligned} \quad (42)$$

where the second term describes the spin-fermion interaction, and  $S_{eff}$  is the action of the effective magnon-paramagnon theory (36). One may represent the spin vector  $\mathbf{S}$  by means of magnons and paramagnons. The partition function can be then written as a path integral over the complex functions of the Matsubara time  $\tau$   $a(\tau, \mathbf{r}), a^+(\tau, \mathbf{r}), \varphi(\tau, \mathbf{r})$  (magnons, paramagnons) and Grassmann functions  $c_\sigma(\tau, \mathbf{r}), c_\sigma^+(\tau, \mathbf{r})$

$$\mathcal{Z}(\beta) = \int D\mu (a^+, a, \varphi, c_\sigma^+, c_\sigma) e^{-S_{s-f}}. \quad (43)$$

In the spin-wave approximation Eqs.(38,39) the effective action  $S_{s-f}$  is quadratic with respect to the spin fluctuations, and one may integrate them out using the formula for the Gaussian integral [55]. As a result one obtains an effective Fermi theory. It is convenient to write the action as a sum  $S_f = S_{f-0} + S_{f-int}$  of a free part

$$S_{f-0} = \int_0^\beta d\tau \int \frac{d^3p}{(2\pi)^3} [c_\sigma^+(\tau, \mathbf{p}) \dot{c}_\sigma(\tau, \mathbf{p}) + \epsilon_\sigma(p) c_\sigma^+(\tau, \mathbf{p}) c_\sigma(\tau, \mathbf{p})], \quad (44)$$

where  $\epsilon_\sigma(p)$  are the dispersions of spin-up and spin-down fermions in ferromagnetic phase.

$$\epsilon_\uparrow(p) = \frac{p^2}{2m} - \mu - \frac{JM}{2}, \quad \epsilon_\downarrow(p) = \frac{p^2}{2m} - \mu + \frac{JM}{2}, \quad (45)$$

and four-fermion interaction resulting from the exchange of spin fluctuations

$$\begin{aligned}
S_{f-int} = & -\frac{J^2}{8} \int d^4x_1 \int d^4x_2 \left[ c_{\uparrow}^+(x_1)c_{\uparrow}(x_1) - c_{\downarrow}^+(x_1)c_{\downarrow}(x_1) \right] \\
& D^{long}(x_1 - x_2) \left[ c_{\uparrow}^+(x_2)c_{\uparrow}(x_2) - c_{\downarrow}^+(x_2)c_{\downarrow}(x_2) \right] \\
& - \frac{J^2}{4} \int d^4x_1 d^4x_2 c_{\downarrow}^+(x_1)c_{\uparrow}(x_1) D^{tr}(x_1 - x_2) c_{\uparrow}^+(x_2)c_{\downarrow}(x_2).
\end{aligned} \tag{46}$$

where  $x = (\tau, \mathbf{r})$ ,  $D^{long}$  is the paramagnon propagator, and  $D^{tr}$  is the magnon Green function Eq.(40).

For the purpose of doing analytical calculations it is convenient to approximate the four-fermion interaction with the static one. To this end I replace the magnon and paramagnon propagators Eq.(40) by static potentials

$$\begin{aligned}
D^{tr}(\omega, \mathbf{p}) & \rightarrow V_m(p) = \frac{2M}{\rho p^2} \\
D^{long}(\omega, \mathbf{p}) & \rightarrow V_{pm}(p) = \frac{1}{r + b p^2}.
\end{aligned} \tag{47}$$

Let us represent the spin anti-parallel composite field  $c_{\uparrow}c_{\downarrow}$  as a sum of symmetric and antisymmetric parts. After some algebra one obtains an effective four fermion theory which can be written as a sum of four terms. Three of them describe the interaction of the components of spin-1 composite fields ( $\uparrow\uparrow, \uparrow\downarrow + \downarrow\uparrow, \downarrow\downarrow$ ). The fourth term describes the interaction of the spin singlet composite fields  $\uparrow\downarrow - \downarrow\uparrow$ . The Hamiltonians of interactions are

$$H_{\uparrow\uparrow} = -\frac{J^2}{8} \int \prod_i \frac{d^3p_i}{(2\pi)^3} \left[ c_{\uparrow}^+(\mathbf{p}_1)c_{\uparrow}^+(\mathbf{p}_2)c_{\uparrow}(\mathbf{p}_2 - \mathbf{p}_3)c_{\uparrow}(\mathbf{p}_1 + \mathbf{p}_3) \right] V_{pm}(\mathbf{p}_3) \tag{48}$$

$$H_{\downarrow\downarrow} = -\frac{J^2}{8} \int \prod_i \frac{d^3p_i}{(2\pi)^3} \left[ c_{\downarrow}^+(\mathbf{p}_1)c_{\downarrow}^+(\mathbf{p}_2)c_{\downarrow}(\mathbf{p}_2 - \mathbf{p}_3)c_{\downarrow}(\mathbf{p}_1 + \mathbf{p}_3) \right] V_{pm}(\mathbf{p}_3) \tag{49}$$

$$\begin{aligned}
H_{\uparrow\downarrow+\downarrow\uparrow} = & -\frac{J^2}{8} \int \prod_i \frac{d^3p_i}{(2\pi)^3} \left[ c_{\uparrow}^+(\mathbf{p}_1)c_{\downarrow}^+(\mathbf{p}_2) + c_{\downarrow}^+(\mathbf{p}_1)c_{\uparrow}^+(\mathbf{p}_2) \right] \\
& \times [c_{\uparrow}(\mathbf{p}_2 - \mathbf{p}_3)c_{\downarrow}(\mathbf{p}_1 + \mathbf{p}_3) + c_{\downarrow}(\mathbf{p}_2 - \mathbf{p}_3)c_{\uparrow}(\mathbf{p}_1 + \mathbf{p}_3)] V_-(\mathbf{p}_3)
\end{aligned} \tag{50}$$

$$\begin{aligned}
H_{\uparrow\downarrow-\downarrow\uparrow} = & \frac{J^2}{16} \int \prod_i \frac{d^3p_i}{(2\pi)^3} \left[ c_{\uparrow}^+(\mathbf{p}_1)c_{\downarrow}^+(\mathbf{p}_2) - c_{\downarrow}^+(\mathbf{p}_1)c_{\uparrow}^+(\mathbf{p}_2) \right] \\
& \times [c_{\uparrow}(\mathbf{p}_2 - \mathbf{p}_3)c_{\downarrow}(\mathbf{p}_1 + \mathbf{p}_3) - c_{\downarrow}(\mathbf{p}_2 - \mathbf{p}_3)c_{\uparrow}(\mathbf{p}_1 + \mathbf{p}_3)] V_+(\mathbf{p}_3),
\end{aligned} \tag{51}$$

where

$$V_-(p) = \frac{2M}{\rho p^2} - \frac{1}{r + b p^2}, \quad V_+(p) = \frac{2M}{\rho p^2} + \frac{1}{r + b p^2}. \tag{52}$$



The spin singlet fields' interaction Eq.(51) is repulsive and does not contribute to the superconductivity[56]. The spin parallel fields' interactions Eqs. (48,49) are mediated by the exchange of longitudinal spin fluctuations and the resulting state is spin-parallel Cooper pairing. The interaction of the  $\uparrow\downarrow + \downarrow\uparrow$  fields Eq.(50) is relevant for magnon-induced superconductivity. It has an attracting part due to exchange of magnons and a repulsive part due to exchange of paramagnons.

### 3.4 Paramagnon exchange mechanism of FM-superconductivity

The most popular theory of FM-superconductivity is based on the paramagnon exchange mechanism[57, 58] with Hamiltonians of interaction Eqs.(48) and (49). By means of the Hubbard-Stratanovich transformation one introduces  $\uparrow\uparrow$  and  $\downarrow\downarrow$  composite fields, the order parameters, and then the fermions can be integrated out. The obtained free energy is a function of the composite fields and the integral over the composite fields can be performed approximately by means of the steepest descend method. To this end one sets the first derivatives of the free energy with respect to composite fields equal to zero, these are the gap equations. To obtain the critical temperature  $T_{sc}$  one considers the finite temperature gap equations linearized at critical temperature[58]

$$\Delta_\sigma(\mathbf{p}) = \frac{1}{2Z^2(0)} \int \frac{d^3k}{(2\pi)^3} V_{pm}(\mathbf{p} - \mathbf{k}) \frac{\tanh(\frac{\beta_{sc}}{2}\epsilon_\sigma^*(\mathbf{k}))}{\epsilon_\sigma^*(\mathbf{k})} \Delta_\sigma(\mathbf{k}). \quad (53)$$

where  $Z(0)$  is the mass renormalization constant  $m^*/m = Z(0)$ . For nearly ferromagnetic system, it scales with magnetization  $M$  like  $Z(0) \sim \ln(1/M)$ [59]. In Eq.(53),  $\epsilon_\sigma^*(\mathbf{p})$  are the spin- $\sigma$  dispersions (45) with  $m \rightarrow m^*$ , and  $\beta_{sc}$  is the inverse critical temperature. To solve the gap equations, one expands the gap functions in spherical harmonics  $Y_{lm}$  and keeps only the  $l = 1, m = 0$  component. Then, the superconducting critical temperature can be obtained following McMillan approximation

$$T_{sc}^\sigma = 1.14\omega(M) \exp[-Z(0)/\lambda_1^\sigma], \quad (54)$$

where

$$\lambda_1^\sigma = \frac{N^\sigma(0)}{2(k_f^\sigma)^2} \int_0^{2k_f^\sigma} dk k \left( 1 - \frac{k^2}{2(k_f^\sigma)^2} \right) V_{pm}(k), \quad (55)$$

$k_f^\sigma$  are the Fermi wavevectors for the spin-up and spin-down Fermi surfaces, and  $N^\sigma(0)$  is the density of states at the spin- $\sigma$  Fermi surface. Near the quantum phase transition ( $M = 0$ ),  $\lambda_1^\sigma$  diverges like  $\ln(1/M)$  and cancels the logarithmic singularity of the renormalization parameter  $Z(0)$ . As a result, the  $M$  dependence of the critical temperature is determined by  $\omega(M)$ . The superconducting transition temperatures as a function of the exchange interaction parameter  $\bar{I}$

are depicted in Fig.5. In the ferromagnetic phase  $\bar{I} > 1$ , and the magnetic transitions occurs at  $\bar{I} = 1$ . The parameter  $r = \bar{I} - 1$  measures the distance from the quantum critical point (see Eqs.(40,41)) and scales with magnetization like  $r \sim M^2$ [41, 46, 49, 53].

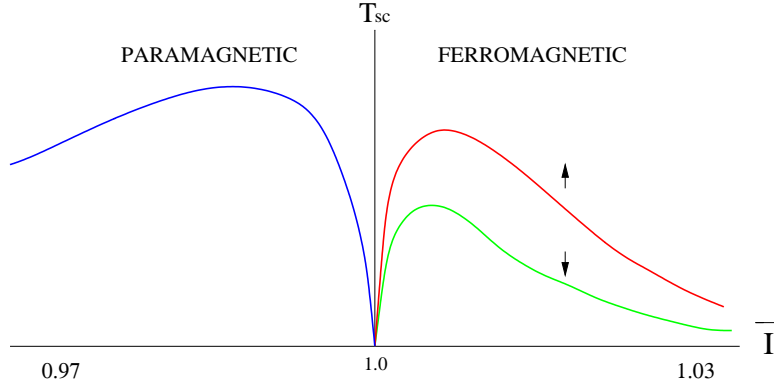


Figure 5: Paramagnon exchange mechanism of superconductivity. The superconducting transition temperature as a function of the exchange interaction parameter  $\bar{I}$ .

In paramagnetic phase the spectrum consists of spin singlet fluctuations of paramagnon type. The exchange of paramagnons leads to a four-fermion interaction, which is attractive in triplet channel. The rotational symmetry, in continual limit, requires all three components ( $\uparrow\uparrow, \uparrow\downarrow + \downarrow\uparrow, \downarrow\downarrow$ ) of the spin-1 vector to be nonequal to zero. The superconducting transition temperature as a function of the exchange interaction parameter  $\bar{I}$  is depicted in Fig.5. In the paramagnetic phase  $\bar{I} < 1$ , and the parameter  $r = 1 - \bar{I}$  measures the distance from the quantum critical point.

The superconducting critical temperature in Fay and Appel theory increases when the magnetization decreases and very close to the quantum critical point falls down rapidly Fig.5. It has recently been the subject of controversial debate. It is obtained in [60], by means of a more complete Eliashberg treatment, that the transition temperature is nonzero at the critical point. In [61], however, the authors have shown that the reduction of quasiparticle coherence and life-time due to spin fluctuations is the pair-breaking process which leads to a rapid reduction of the superconducting critical temperature near the quantum critical point. In order to explain the absence of superconductivity in paramagnetic phase of  $UGe_2$ ,  $URhGe$  and  $ZrZn_2$  it was accounted for the magnon paramagnon interaction and proved that the critical temperature is much higher in the ferromagnetic phase than in the paramagnetic one [62].

Despite of the efforts, the improved theory of paramagnon induced superconductivity can not cover the whole variety of properties of FM superconductivity.

### 3.5 Magnon induced FM superconductivity

Magnon exchange mechanism of superconductivity has been proposed [63] to explain in a natural way the fact that the superconductivity in  $UGe_2$ ,  $ZrZn_2$  and  $URhGe$  is confined to the ferromagnetic phase. The order parameter is a spin anti-parallel component  $\uparrow\downarrow + \downarrow\uparrow$  of a spin-1 triplet ( $\uparrow\uparrow, \uparrow\downarrow + \downarrow\uparrow, \downarrow\downarrow$ ) with zero spin projection. The effective Hamiltonian of the system is

$$H_{eff} = H_0 + H_{\uparrow\downarrow+\downarrow\uparrow} \quad (56)$$

where  $H_0$  is the Hamiltonian of the free spin up and spin down fermions with dispersions Eq.(45) and Hamiltonian of interaction (50). The transverse spin fluctuations are pair forming and the longitudinal ones are pair breaking.

By means of the Hubbard-Stratanovich transformation one introduces composite field  $\uparrow\downarrow + \downarrow\uparrow$  and then the fermions can be integrated out. The integral over the composite field can be performed approximately by means of the steepest descend method. To this end one sets the derivative of the free energy with respect to composite field equal to zero, this is the gap equation. To ensure that the fermions which form Cooper pairs are the same as those responsible for spontaneous magnetization, one has to consider the equation for the magnetization as well.

$$M = \frac{1}{2} \langle c_{\uparrow}^{\dagger} c_{\uparrow} - c_{\downarrow}^{\dagger} c_{\downarrow} \rangle \quad (57)$$

The system of equations for the gap and for the magnetization determines the phase where the superconductivity and the ferromagnetism coexist.

The system can be written in terms of Bogoliubov excitations, which have the following dispersions relations:

$$\begin{aligned} E_1(\mathbf{p}) &= -\frac{JM}{2} - \sqrt{\epsilon^2(\mathbf{p}) + |\Delta(\mathbf{p})|^2} \\ E_2(\mathbf{p}) &= \frac{JM}{2} - \sqrt{\epsilon^2(\mathbf{p}) + |\Delta(\mathbf{p})|^2} \end{aligned} \quad (58)$$

where  $\Delta(\mathbf{p})$  is the gap, and  $\epsilon(\mathbf{p}) = \frac{p^2}{2m} - \mu$ . At zero temperature the equations take the form

$$M = \frac{1}{2} \int \frac{d^3k}{(2\pi)^3} [1 - \Theta(-E_2(\mathbf{k}))] \quad (59)$$

$$\Delta(\mathbf{p}) = \frac{J^2}{8} \int \frac{d^3k}{(2\pi)^3} \frac{V(\mathbf{p}-\mathbf{k}) \Theta(-E_2(\mathbf{k}))}{\sqrt{\epsilon^2(\mathbf{k}) + |\Delta(\mathbf{k})|^2}} \Delta(\mathbf{k}) \quad (60)$$

The gap is an antisymmetric function  $\Delta(-\mathbf{p}) = -\Delta(\mathbf{p})$ , so that the expansion in terms of spherical harmonics  $Y_{lm}(\Omega_{\mathbf{p}})$  contains only terms with odd  $l$ . I assume that the component with  $l = 1$  and  $m = 0$  is nonzero and the other ones are zero

$$\Delta(\mathbf{p}) = \Delta_{10}(p) \sqrt{\frac{3}{4\pi}} \cos \theta. \quad (61)$$

Expanding the potential  $V_-(\mathbf{p} - \mathbf{k})$  in terms of Legendre polynomial  $P_l$  one obtains that only the component with  $l = 1$  contributes the gap equation. The potential  $V_1(p, k)$  has the form,

$$V_1(p, k) = \frac{3M}{\rho} \left[ \frac{p^2 + k^2}{4p^2k^2} \ln \left( \frac{p+k}{p-k} \right)^2 - \frac{1}{pk} \right] - \frac{3M}{\rho} \beta \left[ \frac{p^2 + k^2}{4p^2k^2} \ln \frac{r' + (p+k)^2}{r' + (p-k)^2} - \frac{1}{pk} \right], \quad (62)$$

where  $3M/\rho = 3/\rho_0$ ,  $\beta = \rho/2Mb = \rho_0/2b > 1$  and  $r' = r/b \ll 1$ . A straightforward analysis shows that for a fixed  $p$ , the potential is positive when  $k$  runs an interval around  $p$  ( $p - \Lambda, p + \Lambda$ ), where  $\Lambda$  is approximately independent on  $p$ . In order to allow for an explicit analytic solution, I introduce further simplifying assumptions by neglecting the dependence of  $\Delta_{10}(p)$  on  $p$  ( $\Delta_{10}(p) = \Delta_{10}(p_f) = \Delta$ ) and setting  $V_1(p_f, k)$  equal to a constant  $V_1$  within interval  $(p_f - \Lambda, p_f + \Lambda)$  and zero elsewhere. The system of equations (59,60) is then reduced to the system

$$M = \frac{1}{8\pi^2} \int_0^\infty dk k^2 \int_{-1}^1 dt [1 - \Theta(-E_2(k, t))] \quad (63)$$

$$\Delta = \frac{J^2 V_1}{32\pi^2} \int_{p_f - \Lambda}^{p_f + \Lambda} dk k^2 \int_{-1}^1 dt t^2 \frac{\Theta(-E_2(k, t))}{\sqrt{\epsilon^2(k) + \frac{3}{4\pi} t^2 \Delta^2}} \Delta \quad (64)$$

where  $t = \cos \theta$ .

### 3.5.1 Solution which satisfies $\sqrt{\frac{3}{\pi}} \Delta < JM$

The equation of magnetization (63) shows that it is convenient to represent the gap in the form  $\Delta = \sqrt{\frac{\pi}{3}} \kappa(M) JM$ , where  $\kappa(M) < 1$ . Then the equation

$$E_2(p, t) = 0, \quad (65)$$

defines the Fermi surfaces,

$$p_f^\pm = \sqrt{p_f^2 \pm m \sqrt{J^2 M^2 - \frac{3}{\pi} t^2 \Delta^2}}, \quad p_f = \sqrt{2\mu m} \quad (66)$$

The domain between the Fermi surfaces contributes to the magnetization  $M$  in Eq.(63), but it is cut out from the domain of integration in the gap equation Eq.(64). When the magnetization increases, the domain of integration in the gap equation decreases. Near the quantum critical point the size of the gap is small, and hence the linearized gap equation can be considered. Then it is easy to obtain the critical value of the magnetization  $M_{SC}$  [64].

When the magnetization approaches zero, the domain between the Fermi surfaces decreases. One can approximate the equation for magnetization Eq.(63)

substituting  $p_f^\pm$  from Eq.(66) in the the difference  $(p_f^+)^2 - (p_f^-)^2$  and setting  $p_f^\pm = p_f$  elsewhere. Then, in this approximation, the magnetization is linear in  $\Delta$ , namely

$$\Delta = \sqrt{\frac{\pi}{3}} J \kappa M \quad (67)$$

where  $\kappa$  runs the interval  $(0, 1)$ , and satisfies the equation

$$\kappa \sqrt{1 - \kappa^2} + \arcsin \kappa = \frac{8\pi^2}{mp_f J} \quad (68)$$

The Eq.(68) has a solution if  $mp_f J > 16\pi$ . Substituting  $M$  from Eq.(67) in Eq.(64), one arrives at an equation for the gap. This equation can be solved in a standard way and the solution is

$$\begin{aligned} \Delta &= \sqrt{\frac{16\pi}{3}} \frac{\Lambda p_f \kappa}{m} \exp \left[ -\frac{3}{2} I(\kappa) - \frac{24\pi^2}{J^2 V_1 m p_f} \right] \\ I(\kappa) &= \int_{-1}^1 dt t^2 \ln \left( 1 + \sqrt{1 - \kappa^2 t^2} \right) \end{aligned} \quad (69)$$

Eqs (67,68,69) are the solution of the system Eqs.(63,64) near the quantum transition to paramagnetism.

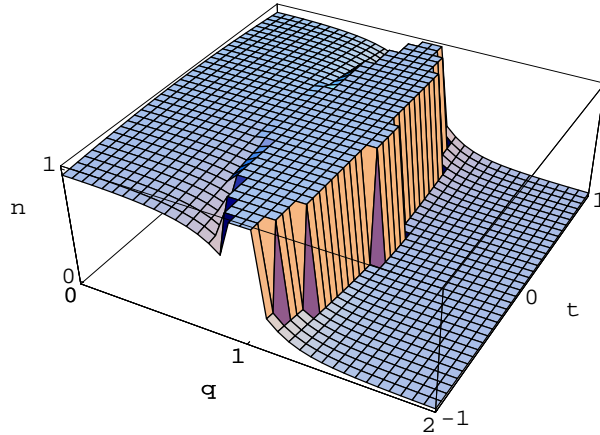


Figure 6: The zero temperature momentum distribution  $n$ , for spin up fermions, as a function of  $q = \frac{p}{p_f}$  and  $t = \cos \theta$ .

One can write the momentum distribution functions  $n^\uparrow(p, t)$  and  $n^\downarrow(p, t)$  of the spin-up and spin-down quasiparticles in terms of the distribution functions of the Bogoliubov fermions

$$\begin{aligned} n^\uparrow(p, t) &= u^2(p, t) n_1(p, t) + v^2(p, t) n_2(p, t) \\ n^\downarrow(p, t) &= u^2(p, t) (1 - n_1(p, t)) + v^2(p, t) (1 - n_2(p, t)) \end{aligned} \quad (70)$$

where  $u(p, t)$  and  $v(p, t)$  are the coefficients in the Bogoliubov transformation. At zero temperature  $n_1(p, t) = 1$ ,  $n_2(p, t) = \Theta(-E_2(p, t))$ , and the Fermi surfaces Eq.(65) manifest themselves both in the spin-up and spin-down momentum distribution functions. The functions are depicted in Fig.6 and Fig.7.

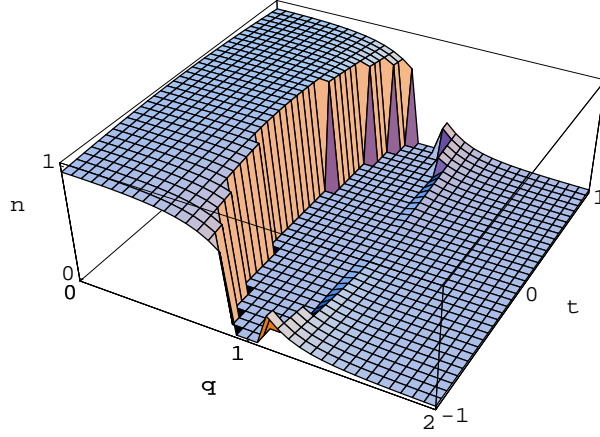


Figure 7: The zero temperature momentum distribution  $n$ , for spin-down fermions, as a function of  $q = \frac{p}{p_f}$  and  $t = \cos \theta$ .

The two Fermi surfaces explain the mechanism of Cooper pairing. In the ferromagnetic phase  $n^\uparrow$  and  $n^\downarrow$  have different (majority and minority) Fermi surfaces (see Fig.8 and Fig.9,  $t = 0$  graphs).

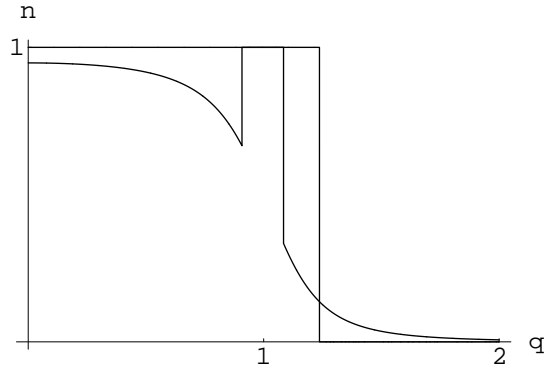


Figure 8: The zero temperature momentum distribution  $n$ , for spin-up fermions, as a function of  $q = \frac{p}{p_f}$  for  $t = 0$  (the gap is zero) and  $t = \pm$  (the gap is maximal).

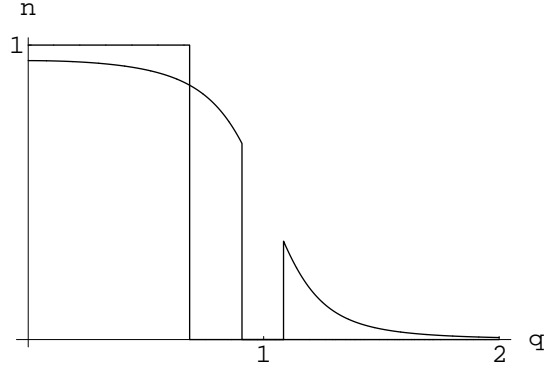


Figure 9: The zero temperature momentum distribution  $n$ , for spin-down fermions, as a function of  $q = \frac{p}{p_f}$  for  $t = 0$  (the gap is zero) and  $t = \pm$  (the gap is maximal).

The spin-up electrons contribute the majority Fermi surface, and spin-down electrons contribute the minority Fermi surface. When the value of the momentum of the emitted or absorbed magnon lies within interval  $(p_f - \Lambda, p_f + \Lambda)$  the effective potential between spin-up and spin-down electrons is attracting. Hence, if the Fermi momenta  $p_f^\uparrow$  and  $p_f^\downarrow$  lie within interval  $(p_f - \Lambda, p_f + \Lambda)$  the interaction between spin-up electrons, which contribute the majority Fermi surface, and spin-down electrons, which contribute the minority Fermi surface, is attracting. As a result, spin-up electrons from majority Fermi surface transfer to the minority Fermi surface and form spin anti-parallel Cooper pairs, while spin-down electrons from minority Fermi surface transfer to the majority one and form spin anti-parallel Cooper pairs too. As a result, the onset of superconductivity is accompanied by the appearance of a second Fermi surface in each of the spin-up and spin-down momentum distribution functions (see Fig.8 and Fig.9,  $t = 1$  graphs).

The existence of the two Fermi surfaces explains the linear dependence of the specific heat at low temperatures:

$$\frac{C}{T} = \frac{2\pi^2}{3} (N^+(0) + N^-(0)) \quad (71)$$

Here  $N^\pm(0)$  are the density of states on the Fermi surfaces. One can rewrite the  $\gamma = \frac{C}{T}$  constant in terms of Elliptic Integral of the second kind  $E(\alpha, x)$

$$\gamma = \frac{mp_f}{3\kappa} \left[ (1+s)^{\frac{1}{2}} E\left(\frac{1}{2} \arcsin \kappa, \frac{2s}{s+1}\right) + (1-s)^{\frac{1}{2}} E\left(\frac{1}{2} \arcsin \kappa, \frac{2s}{s-1}\right) \right], \quad (72)$$

where  $s = JMm/p_f^2 < 1$  and  $\kappa = \sqrt{3/\pi} \Delta/JM$ .

### 3.5.2 Solution which satisfies $\sqrt{\frac{3}{\pi}}\Delta > JM$

In the present sub-chapter one looks for a solution of the system which satisfies

$$\sqrt{\frac{3}{\pi}}\Delta > JM \quad (73)$$

The inequality Eq.(73) shows that the gap can not be arbitrarily small when the magnetization is finite. Hence the system undergoes the quantum phase transition from ferromagnetism to FM-superconductivity with a jump. Approaching the quantum critical point from the ferromagnetic side, one sets the gap equal to zero in the equation for the magnetization (63) and considers the gap equation (64) with magnetization as a parameter. It is more convenient to consider the free energy as a function of the gap for the different values of the parameter  $M$ . To this purpose I introduce the dimensionless "gap"  $x$  and the parameters  $s, \lambda$  and  $g$

$$x = \sqrt{\frac{3}{\pi}} \frac{m}{p_f^2} \Delta, \quad s = \frac{m}{p_f^2} JM, \quad \lambda = \frac{\Lambda}{p_f}, \quad g = \frac{J^2 V_1 m p_f}{8\pi^2} \quad (74)$$

Then the free energy is a function of  $x$  and depends on the parameters  $s, \lambda$  and  $g$ . The dimensionless free energy  $F(x)$  is depicted in Fig.10 for  $\lambda = 0.08$ ,  $g = 20$  and three values of the parameter  $s$ ,  $s = 0.8, s = 0.69$  and  $s_{cr} = 0.595$ .

$$F(x) = \frac{6m^2}{\pi p_f^4} (\mathcal{F}(x) - \mathcal{F}(0)) = x^2 + g \int_{1-\lambda}^{1+\lambda} dq q^2 \int_{-1}^1 dt \times \\ \left[ \left( s - \sqrt{(q^2 - 1)^2 + t^2 x^2} \right) \Theta(\sqrt{(q^2 - 1)^2 + t^2 x^2} - s) - \right. \\ \left. \left( s - \sqrt{(q^2 - 1)^2} \right) \Theta(\sqrt{(q^2 - 1)^2} - s) \right] \quad (75)$$

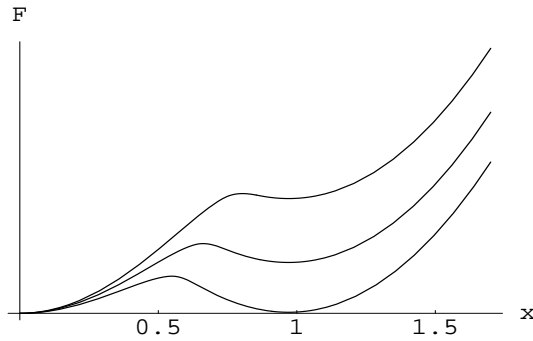


Figure 10: The dimensionless free energy  $F(x)$  as a function of dimensionless gap  $x$ .  $\lambda = 0.08$ ,  $g = 20$ ,  $s_1 = 0.8$ (upper line),  $s_2 = 0.69$ (middle line) and  $s_{cr} = 0.595$ (lower line).



As the graph shows, for some values of the microscopic parameters  $\lambda$  and  $g$ , and decreasing the parameter  $s$  (the magnetization), the system passes through a first order quantum phase transition. The critical values  $s_{cr}$  and  $x_{cr}$  satisfy  $x_{cr}/s_{cr} = \sqrt{3/\pi} \Delta_{cr}/JM_{cr} > 1$  in agreement with Eq.(73).

Varying the microscopic parameters beyond the critical values, one has to solve the system of equations (63,64). One represents again the gap in the form

$$\Delta = \sqrt{\frac{\pi}{3}} \kappa(M) JM \quad (76)$$

but now  $\kappa(M) > 1$ . Then the equation  $E_2(k, t) = 0$ , which defines the Fermi surface, has no solution if  $-1 < t < -1/\kappa(M)$  and  $1/\kappa(M) < t < 1$ , and has two solutions

$$p_f^\pm = \sqrt{p_f^2 \pm m \sqrt{J^2 M^2 - \frac{3}{\pi} t^2 \Delta^2}} \quad (77)$$

when  $-1/\kappa(M) < t < 1/\kappa(M)$ .

The solutions (77) determine the two pieces of the Fermi surface. They stick together at  $t = \pm 1/\kappa(M)$ , so that the Fermi surface is simple connected. The domain between pieces contributes to the magnetization  $M$  in Eq.(63), but it is cut out from the domain of integration in the gap equation Eq.(64). The Fermi surface manifests itself both in the spin-up and spin-down momentum distribution functions. The functions are depicted in Fig.11 and Fig.12.

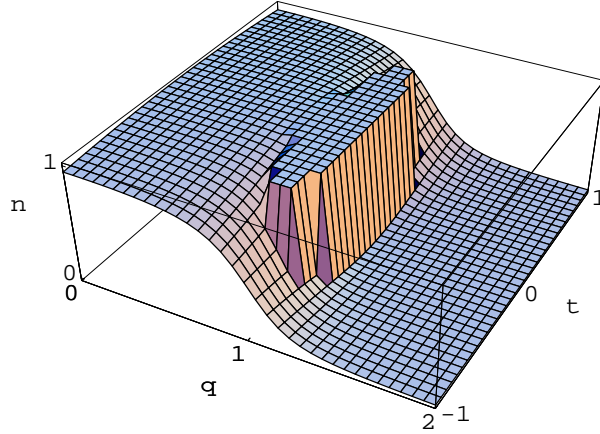


Figure 11: The zero temperature momentum distribution  $n$ , for spin up fermions, as a function of  $q = \frac{p}{p_f}$  and  $t = \cos \theta$ .

When the magnetization approaches zero, one can approximate the equation for magnetization Eq.(63) substituting  $p_f^\pm$  from Eq.(77) in the difference  $(p_f^+)^2 - (p_f^-)^2$  and setting  $p_f^\pm = p_f$  elsewhere. Then, in this approximation, the

magnetization is linear in  $\Delta$ , namely

$$\Delta = \sqrt{\frac{\pi}{3}} J \kappa M \quad (78)$$

where  $\kappa = \frac{mp_f J}{16\pi}$  is the small magnetization limit of  $\kappa(M)$ . The Eq.(78) is a solution if  $mp_f J > 16\pi$  (see Eq.(73)). Substituting  $M$  from Eq.(78) in Eq.(64), one arrives at an equation for the gap. This equation can be solved in a standard way and the solution is

$$\Delta = \sqrt{\frac{16\pi}{3}} \frac{p_f \Lambda}{m} \exp \left[ -\frac{24\pi^2}{mp_f J^2 V_1} - \frac{\pi}{4\kappa^3} + \frac{1}{3} \right] \quad (79)$$

Eqs (78,79) are the solution of the system near the quantum transition to paramagnetism. The second derivative of the free energy Eq.(75) with respect to the gap is positive when  $mp_f J/16\pi > (21\pi/16)^{1/3}$ , hence the state where the superconductivity and the ferromagnetism coexist is stable.

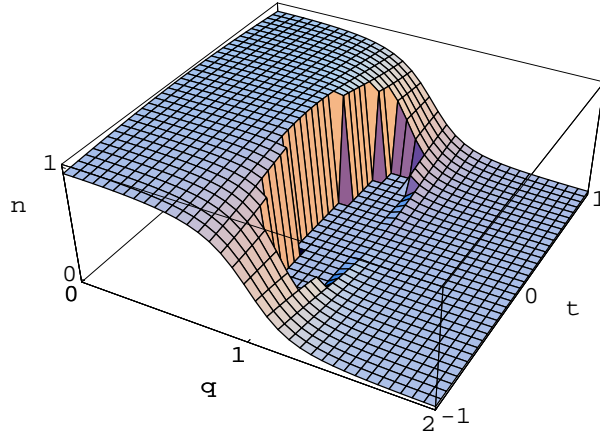


Figure 12: The zero temperature momentum distribution  $n$ , for spin-down fermions, as a function of  $q = \frac{p}{p_f}$  and  $t = \cos \theta$ .

The existence of the Fermi surface explains the linear dependence of the specific heat at low temperature:

$$\frac{C}{T} = \frac{2\pi^2}{3} N(0) \quad (80)$$

Here  $N(0)$  is the density of states on the Fermi surface. One can rewrite the  $\gamma = C/T$  constant in terms of Elliptic Integral of the second kind  $E(\alpha, x)$

$$\gamma = \frac{mp_f}{3\kappa(M)} \left[ (1+s)^{\frac{1}{2}} E\left(\frac{\pi}{4}, \frac{2s}{s+1}\right) + (1-s)^{\frac{1}{2}} E\left(\frac{\pi}{4}, \frac{2s}{s-1}\right) \right], \quad (81)$$

where  $s < 1$ . Eq.(81) shows that for  $\kappa(M)$  just above one the specific heat constant  $\gamma$  is smaller in ferromagnetic phase, while for  $\kappa(M) \gg 1$  it is smaller in FM-superconducting phase. The result closely matches the experiments with  $ZrZn_2$  and  $URhGe$  respectively.

The solutions Eqs.(67,76) show that magnetization and superconductivity disappear simultaneously. It results from the equation of magnetization, which in turn is added to ensure that the fermions which form Cooper pairs are the same as those responsible for spontaneous magnetization. Hence, the fundamental assumption that superconductivity and ferromagnetism are caused by the same electrons leads to the experimentally observable fact that the quantum phase transition is a transition to paramagnetic phase without superconductivity.

An important experimental fact is that  $ZrZn_2$  and  $URhGe$  are superconductors at ambient pressure as opposed to the existence of a quantum phase transition in  $UGe_2$ . To comprehend this difference one considers the potential (62). The quantum phase transition results from the existence of a momentum cutoff  $\Lambda$ , above which the potential is repulsive. In turn, the cutoff existence follows from the relation  $\beta = \rho/2Mb > 1$ , which is true when the spin-wave approximation expression for the spin stiffness constant  $\rho = M\rho_0$  is used. The spin wave approximation correctly describes systems with a large magnetization, for example  $UGe_2$ . But in order to study systems with small magnetization, one has to account for the magnon-magnon interaction which changes the small magnetization asymptotic of  $\rho$ ,  $\rho = M^{1+\alpha}\rho_0$ , where  $\alpha > 0$ . Then for a small  $M$   $\beta < 1$ , and the potential is attractive for all momenta. Hence for systems which, at ambient pressure, are close to quantum critical point, as  $ZrZn_2$  and  $URhGe$ , the magnon self-interaction renormalizes the spin fluctuations parameters so that the magnons dominate the pair formation and quantum phase transition can not be observed. But if one applies an external magnetic field, the magnon opens a gap proportional to the magnetic field. Increasing the magnetic field the paramagnon domination leads to first order quantum phase transition.

The proposed model of ferromagnetic superconductivity differs from the models discussed in [57, 58] in many aspects. First, the superconductivity is due to the exchange of magnons, and the model describes in a unified way the superconductivity in  $UGe_2$ ,  $ZrZn_2$  and  $URhGe$ . Second, the paramagnons have pair-breaking effect. So, the understanding the mechanism of paramagnon suppression is crucial in the search for the ferromagnetic superconductivity with higher critical temperature. For example, one can build such a bilayer compound that the spins in the two layers are oriented in two non-collinear directions, and the net ferromagnetic moment is nonzero. The paramagnon in this phase is totally suppressed and the low lying excitations consist of magnons and additional spin wave modes with linear dispersion  $\epsilon(p) \sim p$ [65]. If the new spin-waves are pair breaking, their effect is weaker than those of the paramagnons, and hence the superconducting critical temperature should be higher. Third, the order parameter is a spin antiparallel component of a spin triplet with zero spin projection. The existence of two Fermi surfaces in each of the spin-up and spin-down

momentum distribution functions leads to a linear temperature dependence of the specific heat at low temperature.

The proposed model of magnon-induced superconductivity does not contain the relativistic effects, namely spin-orbit coupling which is present in  $UGe_2$ . The resulting magneto-crystalline anisotropy will modify the spin-wave excitation and will add a gap in the magnon spectrum, which changes the potential Eq.(62).

## 4 Conclusions

The brief review involves a personal choice of topic and emphasis. Here I have concentrated on the coexistence of ferromagnetism and superconductivity. The main experimental conclusion is that the same band electrons are subject to the ferromagnetic and superconducting instability. The review is devoted to spin exchange mechanism of superconductivity. I have not discussed the phonon mechanism of triple p-type superconductivity[66, 67], the symmetry and nodal structure of the order parameter[68, 69] and other.

The physics of ferromagnetic superconductivity involves a subtle interplay between magnetism and superconductivity. The concept of magnon induced superconductivity is set within the general scheme of itinerant magnetism. It is suggested by the fact that superconducting phase lies entirely in the ferromagnetic one. The theory explains the ferromagnetic to FM-superconducting quantum phase transition and the absence of specific heat anomaly. A point which requires further theoretical investigation is the presence of an additional phase line within ferromagnetic phase. There is no an adequate theoretical explanation of the resistivity anomaly near the characteristic temperature  $T_x$ . Further theoretical work is needed to understand why  $T_x$  decreases with pressure and disappears at a pressure  $p_x$  close to the pressure at which the superconductivity is strongest.

## Acknowledgements

The author would like to thank C. Pfeleiderer, T.M.Rice and C. Honerkamp for valuable discussions. This research is supported by the Sofia University Science Foundation Grant-2003.

## References

- [\*] Electronic address: naoum@phys.uni-sofia.bg
- [1] F.Steglich, J.Aarts, C.D.Bredl, W.Lieke, D.Meschede, W.Franz, and H.Schäfer, Phys.Rev.Lett.,**43**, 1892 (1979).
- [2] H.R.Ott, H.Rudigier, Z.Fisk, and J.L.Smith, Phys.Rev.Lett., **50**, 1595 (1983).

- [3] G.R.Stewart, Z.Fisk, J.O.Willis, and J.L.Smith, Phys.Rev.Lett., **52**, 679 (1984).
- [4] J.L.Smith, J.O.Willis, B.Batlogg, and H.R.Ott, J.Appl.Phys.,**55**, 1996 (1984).
- [5] D.Jerome, D.Mazaud, M.Ribault, K.Bechgaard, J.Physique Lett., **41**, L95, (1980).
- [6] D.Jerome, and H.J.Schulz, Adv.Phys. **51** 293 (2002)[This article is originally published in Adv.Phys. **31** 299 (1982)].
- [7] M.Lang, and J.Müller, Organic Superconductors, arXiv:cond-mat/03 02 157.
- [8] J.G.Bednorz, and K.A.Müller, Z.Phys.,**B 64**, (1986); Rev.Mod.Phys., **60** 585 (1988).
- [9] M.K.Wu, et al., Phys.Rev.Lett., **58**, 908 (1987).
- [10] R.J.Cava, B.Batlogg, K.Kiyano, H.Takagi, J.Krajewski, W.F.Peck, L.W.Rupp, and C.Chen, Phys.Rev.,**49**, 11890 (1994).
- [11] A.A.Abrikosov, L.P.Gorkov, and I.E.Dzyaloshinski, Methods of Quantum Field Theory in Statistical Physics, Dover Publication Inc (1963).
- [12] K. Yosida, Phys.Rev., **110**, 769 (1958).
- [13] L.C.Hebel, and C.P.Slichter, Phys.Rev., **113**, 1504 (1959).
- [14] J.Bardeen, L.N.Cooper, and J.R.Schrieffer, Phys.Rev.,**108**, 1175 (1957).
- [15] D.M.Lee, Rev.Mod.Phys.,**69**, 645 (1997).
- [16] K.Ishida, H.Mukuda, Y.Kitaoka, K.Asayama, Z.Q.Mao, Y.Mori, and Y.Maeno, Nature, **396**, 658 (1998).
- [17] H.Tou, Y.Kitaoka, K.Asayama, N.Kimura, Y.Onuki, E.Yamamoto, and K.Maezawa, Phys. Rev.Lett., **77**, 1374 (1996).
- [18] H.Tou, Y.Kitaoka, K.Ishida, K.Asayama, N.Kimura, Y.Onuki, E.Yamamoto, Y.Haga, and K.Maezawa, Phys.Rev.Lett., **80**, 3129 (1998).
- [19] K.Ishida et.al., Phys.Rev.,**B 56**, R505 (1997).
- [20] G.M.Luke, Y.Fudamoto, K.M.Kojima, M.I.Larkin, J.Merrin, B.Nachumi, Y.J.Uemura, Y.Maeno, Z.Q.Mao, Y.Mori, H.Nakamura, and M.Sigrist, Nature, **394**, 558 (1998).
- [21] S.Adenwella et al.,Phys.Rev.Lett., **65**, 2294 (1990).

- [22] K.Machida and M.Ozaki,Phys.Rev.Lett.,**66**,3293 (1991); T.Ohmi and K.Machida, Phys.Rev.Lett., **71**, 625 (1993).
- [23] T.M.Rice and M.Sigrist, J.Phys.:Condens. Matter **7**, L643 (1995).
- [24] S. Saxena, P. Agarwal, K. Ahilan, F. M. Grosche, R. Haselwimmer, M. Steiner, E. Pugh, I. Walker, S. Julian, P. Monthoux, G. Lonzarich, A. Huxley, I. Sheikin, D. Braithwaite, and J. Flouquet, Nature (London) **406**, 587 (2000).
- [25] C. Pfleiderer, M. Uhlarz, S. Hayden, R. Vollmer, H.v. Löhneysen, N. Bernhoeft, and G. Lonzarich, Nature (London) **412**, 58 (2001).
- [26] D. Aoki, A. Huxley, E. Ressouche, D. Braithwaite, J. Flouquet, J-P. Brison, E.Lhotel, and C. Paulsen, Nature (London) **413**, 613 (2001).
- [27] V.L.Ginzburg, Sov.Phys.JETP, **4**, 153 (1957).
- [28] W.A.Fering, D.C.Johnston, E.DeLong,R.W.McCallum, M.B.Maple, and B.T.Matthias, Phys.Rev.Lett., **38**, 987 (1977).
- [29] D.E.Moncton, D.B.McWahn, P.H.Schmidt, G.Shirane, W.Thomlinson, M.B.Maple, H.B.MacKay, L.D.Woolf, Z.Fisk, and D.C.Johnston, Phys.Rev.Lett., **45**, 2060 (1980).
- [30] M.Ishikawa, and O.Fischer, Solid State Commun. **23**, 37 (1977).
- [31] C.Pfleiderer and H.v.Löhneysen, J.Low Temp.Phys.,**126**, 933 (2002).
- [32] K.Oikawa, T.Kamiyama,T.Asano,Y.Onuki, and M.Kohgi, J.Phys.Soc.Jpn, **65**, 3229 (1996).
- [33] A.B.Shick and W.E.Pickett, Phys.Rev.Lett., **86**, 300 (2001).
- [34] Y.Onuki et al.,J.Phys.Soc.Jpn,**61**, 293 (1992).
- [35] A. Huxley, I. Sheikin, E. Ressouche, N. Kernavanois, D. Braithwaite, R. Calemczuk, and J. Flouquet, Phys. Rev. B **63**, 144519 (2001).
- [36] C. Pfleiderer and A.Huxley, Phys.Rev.Lett., **89**, 147005 (2002).
- [37] N. Tateiwa, T. Kobayashi, K. Hanazono, K. Amaya, Y. Haga, R. Settai, and Y. Onuki, J. Phys. Condens. Matter **13**, L17 (2001).
- [38] H.Yamagami, Physica (Amsterdam) **186B-188B**, 182 (1993).
- [39] J.Flouquet et al.,J.Phys.Soc.Jpn.(Suppl.A), **70**, 14 (2001).
- [40] E. Bauer, R.P.Dickey, V.S.Zapf, and M.B.Maple, J.Phys.:Condens.Matter **13**, L759 (2001).
- [41] G. Lonzarich and L. Taillefer, J. Phys. C **18**, 4339 (1985).

- [42] J. Hubbard, Prog. Roy. Soc. London A **276**, 238 (1963); *ibid* **277**, 237 (1964).
- [43] J. E. Hirsh, Phys.Rev. B **40**, 2354 (1989); *ibid* **40**, 9061 (1989).
- [44] D. Vollhard, N. Blümer, K. Held, M. Kollar, J. Schlipf, and M. Ulmke, Z. Phys. B **103**, 283 (1997).
- [45] A. A. Abrikosov and I. E. Dzyloshinskii, Zh. Eksp. Teor. Fiz. **35**, 771 (1959) [Sov. Phys. JETP. **8**, 535 (1959)].
- [46] I. E. Dzyaloshinskii and P. S. Kondratenko, Zh. Eksp. Teor. Fiz. **70**, 1987 (1974) [Sov. Phys. JETP, **43**, 1036 (1975)].
- [47] K. Murata and S. Doniach, Phys. Rev. Lett. **29**, 285 (1972)
- [48] T. Moriya and A. Kawabata, J. Phys. Soc. Japan **34**, 639
- [49] The works are summarized in T. Moriya, *Spin Fluctuations in Itinerant Electron Magnetism*. (Springer-Verlag, Berlin 1985).
- [50] J. Hertz, Phys. Rev. B **14**, 1165 (1976).
- [51] A. J. Millis, Phys.Rev. B **48**, 7183 (1993).
- [52] D. Schmeltzer, Phys. Rev. B **43**, 8650 (1991).
- [53] N.Karchev, J.Phys.:Condens.Matter **15**, 2797 (2003).
- [54] D.P.Arovas, and A.Auerbach, Phys. Rev. B **38**, 1316 (1988)
- [55] J. W. Negele and H. Orlando, *Quantum Many-Particle Systems* (Addison-Wesley, 1988)
- [56] N. F. Berk, and J. R. Schrieffer, Phys. Rev. Lett. **17**, 433 (1966).
- [57] C. P. Enz, and P. T. Matthias, Science **201**, 828 (1978).
- [58] D. Fay, and J. Appel, Pys.Rev. B **22**, 3173 (1980).
- [59] W.F.Brinkman and S.Engelsberg, Phys.Rev., **169**, 417 (1968).
- [60] R. Roussev and A.Millis, Phys. Rev. B **63**, 140504 (2001).
- [61] Z. Wang, W. Mao, and K. Bedell, Phys. Rev. Lett. **87**, 257001 (2001).
- [62] T. Kirkpatrick, D. Belitz, T. Vojta and R. Narayanan Phys. Rev. Lett. **87**, 127003 (2001).
- [63] N.Karchev, Phys.Rev. B **67**, 054416 (2003).
- [64] N.Karchev, J.Phys.:Condens.Matter **15**, L385 (2003).
- [65] S. Sachdev, and T. Senthila, Ann.Phys.(NY) **251**, 76 (1996).

- [66] A.Abrikosov, J.Phys.:Condens.Matter **13**, L943 (2002).
- [67] H.Suhl, Phys.Rev.Lett.,**87**, 167007 (2001).
- [68] K.Machida, and T.Ohmi, Phys.Rev.Lett. **86**, 850 (2001).
- [69] K.V.Samokhin, and M.B.Walker, Phys.Rev B **66**, 174501 (2002).